Color texture modeling and color image decomposition in a variational-PDE approach

Luminita A. Vese
Department of Mathematics, University of California, Los Angeles
405 Hilgard Avenue, Los Angeles, CA, 90095-1555, U.S.A.
lvese@math.ucla.edu

Stanley J. Osher
Department of Mathematics, University of California, Los Angeles
405 Hilgard Avenue, Los Angeles, CA, 90095-1555, U.S.A.
sjo@math.ucla.edu

Abstract

This paper is devoted to a new variational model for color texture modeling and color image decomposition into cartoon and texture. A given image $\vec{f}$ in the RGB space is decomposed into a cartoon part and a texture part. The cartoon part is modeled by the space of vector-valued functions of bounded variation, while the texture or noise part is modeled by a space of oscillatory functions, dual in some sense of the BV space. Examples for color image decomposition, color image denoising, and color texture discrimination and segmentation will be presented.

1. Introduction

In many problems of image analysis we have an observed color image $\vec{f}$, representing a real scene. The image $\vec{f}$ may contain noise (some random pattern of zero mean for instance) and/or texture (some repeated pattern of small scale details). The image processing task is to extract the most meaningful information from $\vec{f}$. This is usually formulated as an inverse problem: given $\vec{f}$, find another image $\vec{u}$, close to $\vec{f}$, such that $\vec{u}$ is a cartoon or simplification of $\vec{f}$. In general, $\vec{u}$ is an image formed by homogeneous regions and with sharp boundaries. Most models assume the following relation between $\vec{f}$ and $\vec{u}$: $\vec{f} = \vec{u} + \vec{v}$, where $\vec{v}$ is noise or small scale repeated detail (texture), and extract only the $\vec{u}$ component. Usually, the component $\vec{v}$ is not kept, assuming that this models the noise. In this category, we mention Rudin-Osher-Fatemi [28], [14], Mumford-Shah [23], Perona-Malik [26], Alvarez-Guichard-Lions-Morel [1], Chambolle-Lions [8], Aubert-Vese [2], among many others. These models have the ability of computing optimal piecewise-smooth approximations $\vec{u}$ of $\vec{f}$, while noise $\vec{v}$ or small repeated patterns are removed.

Sometimes the $\vec{v}$ component is important, especially if it represents texture, that can be defined as a repeated pattern of small scale details. The noise is also a pattern of small scale details, but of random, uncorrelated values. Both types of patterns (additive noise or texture) can be modeled by oscillatory functions taking both positive and negative values, and of zero mean, as explained by Meyer [24].

Following the ideas of Y. Meyer [24], in a total variation minimization framework of L. Rudin, S. Osher, E. Fatemi (ROF) [28], we show in this paper how we can extract from a color image $\vec{f} = (f_1, f_2, f_3)$ both components $\vec{u} = (u_1, u_2, u_3)$ and $\vec{v} = (v_1, v_2, v_3)$, such that $\vec{u}$ is a function of bounded variation, a cartoon representation of $\vec{f}$, and $\vec{v}$ as texture or noise, is modeled by a space of oscillatory functions, the dual in some sense of the space of functions of bounded variation.

The obtained decomposition can then be useful for segmentation of color textured images and color texture discrimination, among other possible applications. The textured component $\vec{v}$ is completely represented using only two vector-valued functions. This is much simpler and much more efficient than by other techniques for textures, which use a large number of channels to represent a textured image (such as Gabor transform based techniques).

We review next the main two ingredients of the proposed model: the total variation minimization of Rudin-Osher-Fatemi (ROF) [28] for image denoising and restoration (see also Rudin-Osher [27]), and the space of oscillating functions introduced by Y. Meyer [24] to model texture or noise.

Proceedings of the Eighth International Symposium on
Symbolic and Numeric Algorithms for Scientific Computing (SYNASC'06)
0-7695-2740-X/06 $20.00 © 2006 IEEE

Let $\vec{f} = (f_1, f_2, f_3) : \mathbb{R}^2 \to \mathbb{R}^3$ be a given color image in the RGB mode (we assume that the image initially defined on a rectangle in $\mathbb{R}^2$, has been extended to the entire space). We assume that $\vec{f} \in L^2(\mathbb{R}^2, \mathbb{R}^3)$. In real applications, the observed color image $\vec{f}$ is just a noisy version of a true image $\vec{u} = (u_1, u_2, u_3)$, or (as we will see in this paper), it is a textured image, and $\vec{u}$ would be a sketchy approximation or a cartoon image of $\vec{f}$. In the presence of additive noise, the relation between $\vec{u}$ and $\vec{f}$ can be expressed by the linear degradation model, introducing another function $\vec{v}$, and such that $\vec{f}(x, y) = \vec{u}(x, y) + \vec{v}(x, y)$.

In the Rudin-Osher-Fatemi restoration model [28] for gray-scale images, $\vec{v}$ represents noise or small scale repeated details, while $\vec{u}$ is an image formed by homogeneous regions, and with sharp edges. Given $\vec{f}$, both $\vec{u}$ and $\vec{v}$ are unknown (if $\vec{v}$ is noise, we may know some statistics of $\vec{v}$, such that it is of zero mean and given variance). In [28], the problem of reconstructing $\vec{u}$ from $\vec{f}$ is posed as a minimization problem in the space of functions of bounded variation BV, this space allowing for edges or discontinuities along curves. The vector-valued version of their model, efficient for denoising color images while keeping sharp edges, can be expressed as

$$\inf_{\vec{u} \in BV} F(\vec{u}) = \int |\nabla \vec{u}| + \lambda \int |\vec{f} - \vec{u}|^2 dxdy, \qquad (1)$$

where $\lambda > 0$ is a tuning parameter. The first term in the energy, the total variation of $\vec{u}$, is a regularizing term, to remove noise while keeping sharp edges. The second term in the energy is a fidelity term, and $|\cdot|$ denotes the Euclidean norm of a vector in three dimensions. This problem has a unique minimizer in the space $BV(\mathbb{R}^2, \mathbb{R}^3)$ of functions of bounded variation. For $\vec{u} \in L^1(\mathbb{R}^2, \mathbb{R}^3)$, we say that $\vec{u} \in BV(\mathbb{R}^2, \mathbb{R}^3)$ if, and only if,

$$\int |\nabla \vec{u}| = \sup \Big\{ \sum_{i=1}^{3} \int u_i(x, y) \mathrm{div} \vec{g}_i(x, y) dxdy : \vec{g}_i \in C_0^\infty(\mathbb{R}^2, \mathbb{R}^2), |(\vec{g}_1, \vec{g}_2, \vec{g}_3)| \le 1 \Big\} < \infty. \qquad (2)$$

If we denote by $\vec{v} := \vec{f} - \vec{u}$ or $\vec{f} = \vec{u} + \vec{v}$, then the minimization problem (1) can be written as a decomposition

$$\inf_{(\vec{u}, \vec{v})} \Big\{ F(\vec{u}, \vec{v}) = \int |\nabla \vec{u}| + \lambda \| \, |\vec{v}| \, \|_{L^2}^2, \ \vec{f} = \vec{u} + \vec{v} \Big\}. \qquad (3)$$

For $\vec{u} = (u_1, u_2, u_3)$, this can be approximated by

$$\inf_{\vec{u} \in BV} F(\vec{u}) = \int \sqrt{|\nabla u_1|^2 + |\nabla u_2|^2 + |\nabla u_3|^2} + \lambda \sum_{i=1}^{3} \int |f_i - u_i|^2 dxdy. \qquad (4)$$

Formally minimizing the above energy with respect to u_1, u_2 and u_3, we obtain the following system of PDE's:

$$\begin{cases} u_1 = f_1 + \frac{1}{2\lambda} \mathrm{div}\Big(\frac{\nabla u_1}{|\nabla \vec{u}|}\Big), \\ u_2 = f_2 + \frac{1}{2\lambda} \mathrm{div}\Big(\frac{\nabla u_2}{|\nabla \vec{u}|}\Big), \\ u_3 = f_3 + \frac{1}{2\lambda} \mathrm{div}\Big(\frac{\nabla u_3}{|\nabla \vec{u}|}\Big). \end{cases} \qquad (5)$$

Then, the function (residual) representing noise or texture in the vector ROF model is $\vec{v} := \vec{f} - \vec{u}$ given by

$$\vec{v} = -\frac{1}{2\lambda} \Big(\mathrm{div}\Big(\frac{\nabla u_1}{|\nabla \vec{u}|}\Big), \mathrm{div}\Big(\frac{\nabla u_2}{|\nabla \vec{u}|}\Big), \mathrm{div}\Big(\frac{\nabla u_3}{|\nabla \vec{u}|}\Big) \Big),$$

but this is not computed explicitly in the ROF model. Only the component $\vec{u}$ is extracted from $\vec{f}$.

Note that the residual $\vec{v}$ in the ROF model can be formally written as: $v = (\mathrm{div}\vec{g}_1, \mathrm{div}\vec{g}_2, \mathrm{div}\vec{g}_3)$, where $\vec{g}_i = (g_{i,1}, g_{i,2}) = -\frac{1}{2\lambda} \frac{\nabla u_i}{|\nabla \vec{u}|}$. We have that $\sqrt{|\vec{g}_1|^2 + |\vec{g}_2|^2 + |\vec{g}_3|^2} = \frac{1}{2\lambda}$ for all (x, y), therefore $\| \sqrt{|\vec{g}_1|^2 + |\vec{g}_2|^2 + |\vec{g}_3|^2} \|_{L^\infty} = \frac{1}{2\lambda}$.

In [24], Meyer shows that the ROF model does not always separate well texture from BV components. In order to better extract both the $\vec{u}$ component in BV and the $\vec{v}$ component as an oscillating function (texture or noise) from $\vec{f}$, Meyer [24] proposes the use for $\vec{v}$ of a space of functions, which is in some sense the dual of the BV space (this is also motivated by the expression above of the residual $\vec{v}$, and by the condition (2)). In [24] the author considers the scalar case only. Here, we will adapt some of the definitions and terminology introduced in [24] to the vector case.

Definition. *Let G denote the Banach space consisting of all generalized vector-valued functions $\vec{v}(x, y) = (v_1(x, y), v_2(x, y), v_3(x, y))$ which can be written as*

$$\vec{v}(x, y) = (\mathrm{div}\vec{g}_1, \mathrm{div}\vec{g}_2, \mathrm{div}\vec{g}_3), \qquad (6)$$
$$g_{i,1}, g_{i,2} \in L^\infty(\mathbb{R}^2), \ i = 1, 2, 3,$$

induced by the norm $\|v\|_*$ defined as the lower bound of all L^∞ norms of functions $|\vec{g}|$, where $\vec{g} = (\vec{g}_1, \vec{g}_2, \vec{g}_3)$, $|\vec{g}| = \sqrt{|\vec{g}_1|^2 + |\vec{g}_2|^2 + |\vec{g}_3|^2} = \sqrt{\sum_{i=1}^{3} (g_{i,1}^2 + g_{i,2}^2)}$, and where the infimum is computed over all decompositions (6) of $\vec{v}$.

Meyer shows (in the scalar case) that, if the $\vec{v}$ component represents texture or noise, then $\vec{v} \in G$, and proposes the following new image restoration model:

$$\inf_{\vec{u} \in BV} \Big\{ E(\vec{u}) = \int |\nabla \vec{u}| + \lambda \|\vec{v}\|_*, \ \vec{f} = \vec{u} + \vec{v} \Big\}. \qquad (7)$$

We shall see that the space G allows for oscillating functions $\vec{v}$, and the oscillations are well measured by the norm $\|v\|_*$. This norm also helps to discriminate between two different textures of the same average.

However, it is not clear how to solve in practice the minimization problem (7). The main contribution of this present

Proceedings of the Eighth International Symposium on
Symbolic and Numeric Algorithms for Scientific Computing (SYNASC'06)
0-7695-2740-X/06 $20.00 © 2006 IEEE

paper, as described in the next section, is to propose a practical algorithm to solve (7), making use only of simple partial differential equations. We consider here the vector case of color images in the RGB mode. The proposed model for color image decomposition and texture modeling is also an extension from gray-scale to color images of the model introduced in [35], [36].

Other work for restoration of textured images by total variation minimization in a wavelet framework are by F. Malgouyres [20], [21], [22], E.J. Candès and F. Guo [6]. Also, texture modeling by statistical methods was proposed by S.C. Zhu, Y.N. Wu and D. Mumford, in [37], [38], and by S. Casadei, S. Mitter and P. Perona in [7]. In the context of texture segmentation, we cite only a few related work, such as G. Koepfler, C. Lopez, J.-M. Morel [17], G. Sapiro [30], T.S. Lee, D. Mumford, A. Yuille [19], T.S. Lee [18], C. Ballester and M. Gonzalez [4], N. Paragios and R. Deriche [25], R. Kimmel, R. Malladi and N. Sochen [15], among many others. A recent work for segmentation of textured images using segmentation based active contour models in a Gabor transform framework, is proposed by B. Sandberg, T. Chan and L. Vese [29]. Another recent work for image decomposition of color images in the same framework, most relevant to the present paper, is by Aujol-Kang [3]. Prior work on color image restoration, denoising and processing of vector-valued data is by Blomgren and Chan [5], Chan and Kang [9], Kimmel and Sochen [16], Sapiro and Ringach [31], Tang, Sapiro, and Caselles [32], Trahanias et al. [33], Vese and Osher [34], Chan and Shen [11], among many others.

2. Description of the model

We are motivated by the following approximation to the L^∞ norm of $|\vec{g}| = \sqrt{|\vec{g}_1|^2+|\vec{g}_2|^2+|\vec{g}_3|^2} = \sqrt{\sum_{i=1}^3 (g_{i,1}^2+g_{i,2}^2)}$, for $g_{i,1}, g_{i,2} \in L^\infty(\mathbb{R}^2)$:

$$\begin{aligned} &\|\sqrt{|\vec{g}_1|^2+|\vec{g}_2|^2+|\vec{g}_3|^2}\|_{L^\infty} \\ &= \lim_{p\to\infty} \|\sqrt{|\vec{g}_1|^2+|\vec{g}_2|^2+|\vec{g}_3|^2}\|_{L^p}. \end{aligned}$$

Then, we propose the following minimization problem, inspired by (7) and [35], in the vector case:

$$\begin{aligned} \inf_{\vec{u},\vec{g}} G_p(\vec{u},\vec{g}) &= \int |\nabla \vec{u}| \\ &+ \lambda \sum_{i=1}^3 \int |f_i - u_i - \mathrm{div}\vec{g}_i|^2 dxdy \qquad (8) \\ &+ \mu \Big[\int \Big(\sqrt{|\vec{g}_1|^2+|\vec{g}_2|^2+|\vec{g}_3|^2} \Big)^p dxdy \Big]^{\frac{1}{p}}, \end{aligned}$$

where $\lambda, \mu > 0$ are tuning parameters, and $p \to \infty$. Recall that $\vec{u} = (u_1, u_2, u_3)$, and $\vec{g} = (\vec{g}_1, \vec{g}_2, \vec{g}_3)$ with $\vec{g}_i = (g_{i,1}, g_{i,2})$, for $i = 1, 2, 3$.

The first term in (8) insures that $\vec{u} \in BV(\mathbb{R}^2, \mathbb{R}^3)$, the second term insures that $\vec{f} \approx \vec{u} + (\mathrm{div}\vec{g}_1, \mathrm{div}\vec{g}_2, \mathrm{div}\vec{g}_3)$, while the third term is a penalty on the norm $\|\vec{v}\|_*$ of $\vec{v}$ in G. Clearly, if $\lambda \to \infty$ and $p \to \infty$, this model is formally an approximation of (7).

Formally minimizing the above energy (8) with respect to $\vec{u}$ and $\vec{g}$, yields the following system of coupled Euler-Lagrange equations, for $i = 1, 2, 3$:

$$u_i = f_i - \mathrm{div}\vec{g}_i + \frac{1}{2\lambda}\mathrm{div}\Big(\frac{\nabla u_i}{|\nabla \vec{u}|}\Big), \qquad (9)$$

$$\mu \Big(\| \, |\vec{g}| \, \|_p \Big)^{1-p} |\vec{g}|^{p-2} g_{i,1} =$$

$$2\lambda \Big[\frac{\partial}{\partial x}(u_i - f_i) + \partial^2_{xx} g_{i,1} + \partial^2_{xy} g_{i,2} \Big], \qquad (10)$$

$$\mu \Big(\| \, |\vec{g}| \, \|_p \Big)^{1-p} |\vec{g}|^{p-2} g_{i,2} =$$

$$2\lambda \Big[\frac{\partial}{\partial y}(u_i - f_i) + \partial^2_{xy} g_{i,1} + \partial^2_{yy} g_{i,2} \Big]. \qquad (11)$$

In our numerical calculations, we have tested the model for different values of p, with $1 \le p \le 10$. The obtained results were very similar. The case $p = 1$ yields faster calculations per iteration, so we give here the form of the Euler-Lagrange equations in this case $p = 1$. Also, the numerical results presented in the next section have been obtained for $p = 1$. For $i = 1, 2, 3$:

$$u_i = f_i - \partial_x g_{i,1} - \partial_y g_{i,2} + \frac{1}{2\lambda}\mathrm{div}\Big(\frac{\nabla u_i}{|\nabla \vec{u}|}\Big) \qquad (12)$$

$$\mu \frac{g_{i,1}}{|\vec{g}|} = 2\lambda \Big[\frac{\partial}{\partial x}(u_i - f_i) + \partial^2_{xx} g_{i,1} + \partial^2_{xy} g_{i,2} \Big] \qquad (13)$$

$$\mu \frac{g_{i,2}}{|\vec{g}|} = 2\lambda \Big[\frac{\partial}{\partial y}(u_i - f_i) + \partial^2_{xy} g_{i,1} + \partial^2_{yy} g_{i,2} \Big]. \qquad (14)$$

As we shall see in the section devoted to numerical results, the proposed minimization model (8), in the simpler case $p = 1$, allows to extract from a given real color textured image $\vec{f}$ the components $\vec{u} \in BV(\mathbb{R}^2, \mathbb{R}^3)$ and $\vec{v} \in G$, such that $\vec{u}$ is a sketchy (cartoon) approximation of $\vec{f}$, and $\vec{v} = (\mathrm{div}\vec{g}_1, \mathrm{div}\vec{g}_2, \mathrm{div}\vec{g}_3)$ represents the texture or the noise. In addition, the minimizer obtained for $\vec{g} = (\vec{g}_1, \vec{g}_2, \vec{g}_3)$ allows us to discriminate between two different textures of the same intensity average, by looking at one of the RGB images given by $(|g_{1,1}|, |g_{2,1}|, |g_{3,1}|)$, $(|g_{1,2}|, |g_{2,2}|, |g_{3,2}|)$, or at one of the gray-scale images $|g_{1,1}| + |g_{2,1}| + |g_{3,1}|$ or $|g_{1,2}| + |g_{2,2}| + |g_{3,2}|$ (recall that the functions $g_{i,1}$ and $g_{i,2}$, for $i = 1, 2, 3$ compose the norm $\|v\|_*$). We will see that no apriori knowledge or statistical information about the texture is needed.

3. Numerical results and comparisons

We present numerical results obtained with the proposed color decomposition algorithm with $p = 1$ from (12)-(14)

Proceedings of the Eighth International Symposium on
Symbolic and Numeric Algorithms for Scientific Computing (SYNASC'06)
0-7695-2740-X/06 $20.00 © 2006 IEEE

on real images. We show comparisons with the color TV model (3)-(5), and with the method that produces a cartoon component u (piecewise-constant) introduced in [10], based on Mumford-Shah piecewise-smooth approximations [23].

Each time, from a given color image $\vec{f}$, we extract the cartoon part $\vec{u}$ and the texture+noise part $\vec{v}$. For display purposes only, instead of $\vec{v}$, which is a function with very small maximum norm and taking both positive and negative values, we show $150 + \vec{v}$ (the constant 150 has been added to all three components of the vector-valued function $\vec{v}$). We illustrate three applications of the proposed model: color image decomposition into cartoon and texture, color image denoising, and color texture discrimination and segmentation. The above Euler-Lagrange equations (5), (12)-(14) have been discretized and solved using finite differences and fixed-point approximation.

We begin with a color image, a painting of Van Gogh. We show in Fig. 1 the input data $\vec{f}$, and the components $\vec{u}$ and $\vec{v}$ of the decomposition. We note that, as expected, the image $\vec{u}$ is a cartoon representation of the given image $\vec{f}$, while $\vec{v}$ contains the textured small details.

In the next example from Figure 2, the initial color image $\vec{f}$ is noisy. The obtained component $\vec{u}$ is a denoised cartoon approximation of $\vec{f}$, while the component $\vec{v}$ contains texture and noise, together with other small details. We also show comparison with the color TV model (3)-(5). The new model gives a slightly smaller root mean square error, thus an improved result.

In Fig. 3, we perform the same experiment on a color image of an object with fractal boundaries. This image is decomposed into a cartoon image $\vec{u}$ of the object, with smaller perimeter than initially, and an image $\vec{v}$ which contains the oscillations on the boundary only. We also show comparisons with the color TV model (3)-(5) in Fig. 4 and with a cartoon segmentation model from [10] in Fig. 5.

We end the paper with numerical results on a wood textured image shown in Fig. 6. We show the $\vec{u}$ and $\vec{v} := \vec{f} - \vec{u}$ components obtained by the color TV model (3)-(5) in Fig. 7, and with the new model in Fig. 8. We choose here the parameter λ in each case such that the $\vec{v}$ components have the same L^2 norm. Note how the color TV model keeps more texture in the $\vec{u}$ component.

In this experiment, we also show that the obtained vector-valued function $(\vec{g}_1, \vec{g}_2, \vec{g}_3)$, which is such that $\vec{v} = (\mathrm{div}\vec{g}_1, \mathrm{div}\vec{g}_2, \mathrm{div}\vec{g}_3)$ helps to discriminate between two different textures with the same intensity average. Indeed, we show $|g_{1,1}| + |g_{2,1}| + |g_{3,1}|$ as a "texture discriminator', that is segmented by the active contour model without edges [12], [13]. The detected boundary is shown in Fig. 9.

Other expressions function of $\vec{g}$ could have been used for texture discriminators, some involving the gradient magnitude of $\vec{g}$. We do not guarantee that with such texture discriminators we would be able to distinguish between all types of different textures. We plan to investigate this further in the future. But this representation for textured images is more efficient than, for instance, the techniques based on the Gabor transform [29]. In that case, the Gabor transform is applied to the initial image $\vec{f}$, producing a large number of channels corresponding to different parameters, which are then used in a vector-valued segmentation process.

Figure 1. Color decomposition (12)-(14): top, initial image $\vec{f}$; middle, cartoon component $\vec{u}$; bottom, texture component $\vec{v}$.

Proceedings of the Eighth International Symposium on
Symbolic and Numeric Algorithms for Scientific Computing (SYNASC'06)
0-7695-2740-X/06 $20.00 © 2006 IEEE

Figure 2. Top to bottom: original, noisy; $\vec{u}$ and $\vec{f} - \vec{u}$ by the new model (12)-(14) with RMSE = 0.353576; $\vec{u}$ and $\vec{f} - \vec{u}$ by the color TV model (3)-(5) with RMSE = 0.355378.

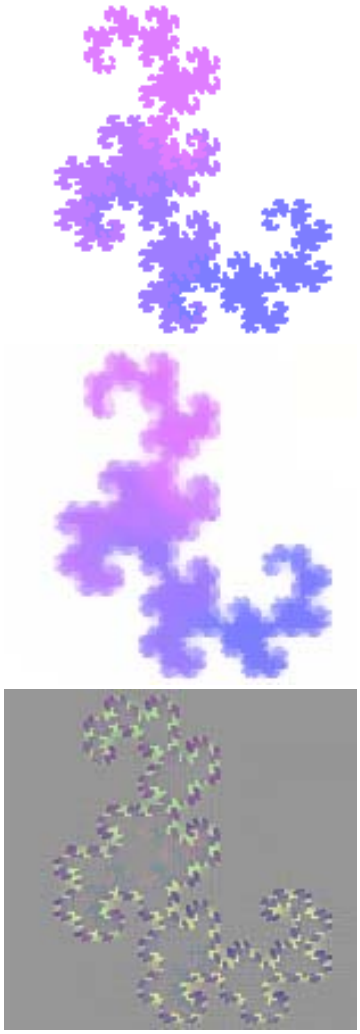

Figure 3. Color image decomposition of an object with fractal boundaries. Top: original $\vec{f}$. Middle: component $\vec{u}$, representing an object with finite perimeter. Bottom: component $\vec{v}$, showing boundary oscillations.

Proceedings of the Eighth International Symposium on
Symbolic and Numeric Algorithms for Scientific Computing (SYNASC'06)
0-7695-2740-X/06 $20.00 © 2006 IEEE

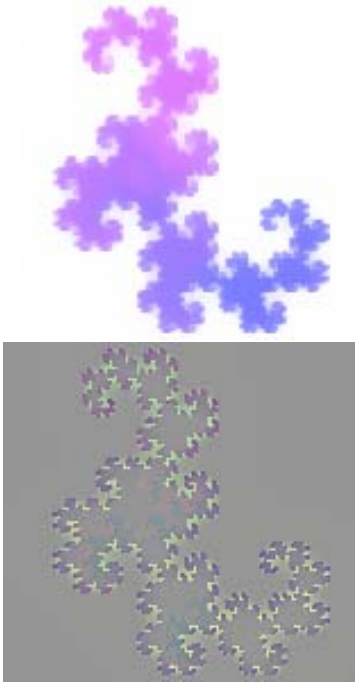

Figure 4. Color TV (3)-(5) applied to the fractal image: components $\vec{u}$, $\vec{v} = \vec{f} - \vec{u}$.

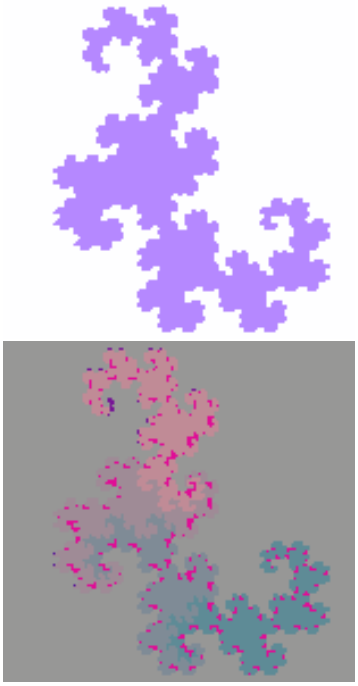

Figure 5. Color cartoon model [10] applied to the fractal image: components $\vec{u}$, $\vec{v} = \vec{f} - \vec{u}$.

Figure 6. $\vec{f}$ with two different wood textures.

Figure 7. Color TV model (3)-(5) applied to the wood image: $\vec{u}$ and $\vec{v}$ components.

Proceedings of the Eighth International Symposium on
Symbolic and Numeric Algorithms for Scientific Computing (SYNASC'06)
0-7695-2740-X/06 $20.00 © 2006 IEEE

Figure 8. $\vec{u}$, $\vec{v}$ components of the color decomposition (12)-(14) for to the wood image.

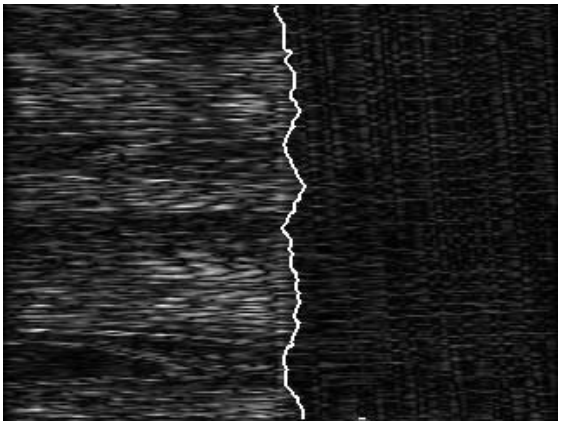

Figure 9. Texture segmentation: application of the active contour model without edges [12], [13] to the gray-level image given by $|g_{1,1}| + |g_{2,1}| + |g_{3,1}|$.

3.1. Conclusions

In this paper, we have proposed a new formulation to model real color textured images, inspired by Y. Meyer, in a vector total variation minimization framework of L. Rudin, S. Osher and E. Fatemi. A given color image is decomposed into a cartoon part and a texture+noise part. The cartoon part is modeled by functions of bounded variation, while the texture+noise part is modeled by oscillatory functions. Examples of color image decomposition, color image denoising and color texture segmentation have been presented, together with comparisons with two related models.

References

[1] L. Alvarez, F. Guichard, P.L. Lions, J.M. Morel. Axioms and fundamental equations of image-processing. *Archive for Rat. Mech. and An.*, 123(3): 199-257, 1993.

[2] G. Aubert, L. Vese. A variational method in image recovery. *SIAM J. on Num. Anal.*, 34(5): 1948-1979, 1997.

[3] J.F. Aujol, S.H.Kang. Color image decomposition and restoration. *JVCIR*, 17(4): 916-928, 2006.

[4] C. Ballester, M. Gonzalez. Affine invariant texture segmentation and shape from texture by variational methods. *JMIV*, 9(2): 141-171, 1998.

[5] P. Blomgren, T.F. Chan. Color TV: Total variation methods for restoration of vector-valued images. *IEEE TIP*, 7(3): 304-309, 1998.

[6] E.J. Candès, F. Guo. New Multiscale Transforms, Minimum Total Variation Synthesis: Applications to Edge-Preserving Image Reconstruction. *Signal Processing*, 82: 1519-1543, 2002.

[7] S. Casadei, S. Mitter, P. Perona. Boundary detection in piecewise homogeneous textured images. *LNCS*, 588: 174-183, 1992.

[8] A. Chambolle, P.L. Lions. Image recovery via total variation minimization and related problems. *Numer. Math.*, 76: 167-188, 1997.

[9] T.F. Chan, S.H. Kang. Total variation denoising and enhancement of color images based on the CB and HSV color models. *JVCIR*, 12(4): 422-435, 2001.

[10] T.F. Chan, B.Y. Sandberg, L.A. Vese. Active contours without edges for vector-valued images. *JVCIR*, 11(2): 130-141, 2000.

[11] T. Chan, J.H. Shen. Variational restoration of nonflat image features: Models and algorithms. *SIAM J. on Applied Maths.*, 61(4): 1338-1361 2000.

Proceedings of the Eighth International Symposium on
Symbolic and Numeric Algorithms for Scientific Computing (SYNASC'06)
0-7695-2740-X/06 $20.00 © 2006 IEEE

[12] T. Chan, L. Vese. An active contour model without edges. *LNCS*, 1682: 141-151, 1999.

[13] T.F. Chan, L.A. Vese. Active contours without edges. *IEEE TIP*, 10(2): 266-277, 2001.

[14] S. Geman, D. Geman. Stochastic relaxation, Gibbs distributions, and the Bayesian restoration of images. *IEEE TPAMI*, 6(6): 721-741, 1984.

[15] R. Kimmel, R. Malladi, N. Sochen. Images as embedded maps and minimal surfaces: Movies, color, texture, and volumetric medical images. *IJCV*, 39(2): 111-129, 2000.

[16] R. Kimmel, N. Sochen. Orientation diffusion or how to comb a porcupine. *JVCIR*, 13(1-2): 238-248, 2002.

[17] G. Koepfler, C. Lopez, J.M. Morel. A multiscale algorithm for image segmentation by variational method. *SIAM J. Num. Anal.*, 31(1): 282-299, 1994.

[18] T.S. Lee. A Bayesian framework for understanding texture segmentation in the primary visual-cortex. *Vision Research*, 35(18): 2643-2657, 1995.

[19] T.S. Lee, D. Mumford, A. Yuille. Texture segmentation by minimizing vector-valued energy functionals - the coupled-membrane model. *LNCS*, 588: 165-173, 1992.

[20] F. Malgouyres. Mathematical analysis of a model which combines total variation and wavelet for image restoration. *Journal of information processes*, 2(1): 1-10, 2002.

[21] F. Malgouyres. Combining total variation and wavelet packet approaches for image de-blurring. *Proceedings, IEEE Workshop on VLSM in Computer Vision*, 57-64, 2001.

[22] F. Malgouyres. Minimizing the total variation under a general convex constraint for image restoration. *IEEE TIP*, 11(12): 1450-1456, 2002.

[23] D. Mumford, J. Shah. Optimal approximations by piecewise smooth functions and associated variational-problems. *Communications on Pure and Appl. Maths.*, 42(5): 577-685, 1989.

[24] Y. Meyer. *Oscillating Patterns in Image Processing and Nonlinear Evolution Equations*. AMS 22, 2002.

[25] N. Paragios, R. Deriche. Geodesic active regions and level set methods for supervised texture segmentation. *IJCV*, 46(3): 223-247, 2002.

[26] P. Perona, J. Malik. Scale-space and edge-detection using anisotropic diffusion. *IEEE TPAMI*, 12(7): 629-639, 1990.

[27] L. Rudin, S. Osher. Total variation based image restoration with free local constraints. *Proc. IEEE ICIP Austin, Texas*, I 31-35, 1994.

[28] L. Rudin, S. Osher, E. Fatemi. Nonlinear total variation based noise removal algorithms. *Physica D*, 60: 259-268, 1992.

[29] B. Sandberg, T. Chan, L. Vese. A Level-Set and Gabor-Based Active Contour Algorithm for Segmenting Textured Images. *UCLA CAM Report* 02-39, 2002.

[30] G. Sapiro. Color Snakes. *CVIU*, 68(2): 247-253, 1997.

[31] G. Sapiro, D. Ringach. Anisotropic diffusion of multivalued images with applications to color filtering. *IEEE TIP*, 5(11): 1582-1586, 1996.

[32] B. Tang, G. Sapiro, V. Caselles. Color image enhancement via chromaticity diffusion. *IEEE TIP*, 10(5): 701-707, 2001.

[33] P.E. Trahanias, D. Karakos, A.N. Venetsanopoulos. Directional processing of color images: Theory and experimental results. *IEEE TIP*, 5(6): 868-880, 1996.

[34] L.A. Vese, S.J. Osher. Numerical methods for p-harmonic flows and applications to image processing. *SIAM J. of Num. Anal.*, 40(6): 2085-2104, 2003.

[35] L.A. Vese, S.J. Osher. Modeling textures with total variation minimization and oscillating patterns in image processing. *JSC*, 19(1-3): 553-572, 2003.

[36] L.A. Vese and S.J. Osher. Image denoising and decomposition with total variation minimization and oscillatory functions. *JMIV*, 20(1-2): 7-18, 2004.

[37] S.C. Zhu, Y.N. Wu, D. Mumford. Filters, random fields and maximum entropy (FRAME): Towards a unified theory for texture modeling. *IJCV*, 27(2): 107-126, 1998.

[38] S.C. Zhu, Y.N. Wu, D. Mumford. Minimax entropy principle and its application to texture modeling. *Neural Computation*, 9(8): 1627-1660, 1997.

Proceedings of the Eighth International Symposium on
Symbolic and Numeric Algorithms for Scientific Computing (SYNASC'06)
0-7695-2740-X/06 $20.00 © 2006 IEEE